

# Neural Architecture Search for Energy Efficient Always-on Audio Models

Daniel T. Speckhard  
X, The Moonshot Factory  
Mountain View, California, USA  
speckhard@fhi.mpg.de

Karolis Misiunas  
Google Research  
Zürich, Switzerland  
kmisiunas@google.com

Sagi Perel  
Google Research  
Mountain View, California, USA  
sagipe@google.com

Tenghui Zhu  
Google Research  
Mountain View, California, USA  
ztenghui@google.com

Simon Carlile  
X, The Moonshot Factory  
Mountain View, California, USA  
carlile.simon@gmail.com

Malcolm Slaney  
Google Research  
Mountain View, California, USA  
malcolm@ieee.org

## ABSTRACT

Mobile and edge computing devices for always-on audio classification require energy-efficient neural network architectures. We present a neural architecture search (NAS) that optimizes accuracy, energy efficiency and memory usage. The search is run on Vizier, a black-box optimization service. We present a search strategy that uses both Bayesian and regularized evolutionary search with particle swarms, and employs early-stopping to reduce the computational burden. The search returns architectures for a sound-event classification dataset based upon AudioSet with similar accuracy to MobileNetV1/V2 implementations but with an order of magnitude less energy per inference and a much smaller memory footprint.

## KEYWORDS

neural architecture search, sound event classification

## 1 INTRODUCTION

It is challenging for the hearing impaired to identify important sounds such as running water, dogs barking, and crying babies. Sound event classification systems feed spectrograms into image classification networks with great results [8]. Much of the sound-event classification work focuses on a paradigm where audio is sent over an Internet connection to a large neural network (such as ResNet50 [7] with 20+ million parameters) that classifies the sound in the cloud. This approach relies on good Internet data speeds. We instead search for a neural network that runs locally for a full day, continuously, on a battery powered device (e.g. smart watch, earphones, phone). This requires a energy efficient network to avoid draining the battery of the device prematurely and a small enough network to be able to fit into device memory.

Much of the platform aware neural architecture search (NAS) literature has focused on inference time (latency) as a user experience requirement for image classification. Instead we think energy usage is the more important limiting factor.

An always-on audio model calculating an inference once every second makes 86400 inferences per day. As a result, the energy required per model inference is a critical matter when searching for the best architecture. A smartphone might have a battery capacity of around 51 kJ (e.g. Google Pixel 4 XL), a smartwatch around 3.6 kJ (e.g. Fitbit Versa 3) and earphones around 0.7 kJ, (e.g. Pixel

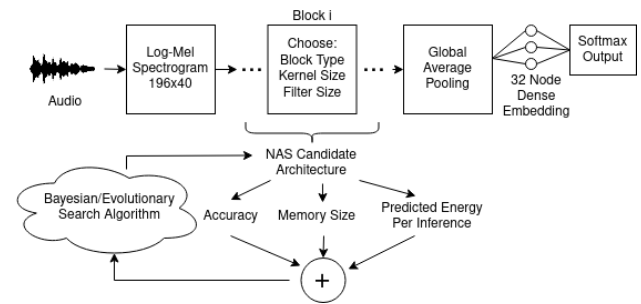
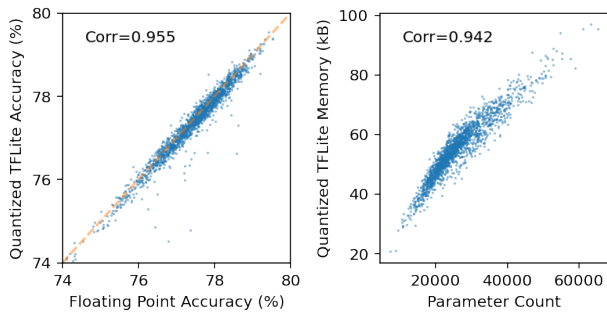


Figure 1: A block diagram of our network architecture search process.

Buds 2). For comparison, the baseline solution of deploying a high-performance network like MobileNetV2 [16] on a Pixel 4 XL big core CPU uses 14 mJ per inference (1.21 kJ per day) when running sound event classification on spectrograms. It’s evident that a network of that size will quickly consume a high fraction of the computing device’s battery capacity.

We present a simple to implement neural architecture search that targets on device energy efficiency, low memory usage for always-on audio models to satisfy the constraints outlined above. Our main contributions are:

- We evaluate our method on a MobileNet based search space and find a model with accuracy slightly better than MobileNetV2 with 10x less energy usage, and 50x smaller memory footprint (Table 1).
- We show FLOPs are not a good proxy for energy usage even on a mobile CPU. Inference time (latency) is a better but imperfect proxy for energy usage. This is because power usage is not consistent across neural networks—memory access and arithmetic operations differ in power (Figure 3).
- We identified a computational bottleneck created by combining spectrograms with 2D convolutional blocks (Table 2). We show that an alternative approach of swapping the frequency axis with the depth axis of the spectrogram and using 1D convolutional blocks reduces energy usage, but underperforms on the accuracy metric.



**Figure 2: Quantized network performance.** Left: Categorical accuracy versus int-8 quantized TFLite accuracy for two thousand candidate architectures sampled by the Vizier Bayesian (hybrid) algorithm. Right: The parameter count plotted against the quantized TFLite memory size.

## 2 OPTIMIZATION CRITERIA

We need to find a balance between energy efficiency and small memory footprint, while still achieving state of the art accuracy. Thus we combine these optimization constraints into a single objective via a weighted sum. The reward proportionally penalizes larger memory sizes and energy usages.

$$R = \text{ACC}(h(x)) - b \max(0, \text{ENERGY}(h) - E_0) - c \max(0, \text{MEM}(h) - M_0) \quad (1)$$

Here  $x$  is the evaluation dataset,  $\text{ACC}$  is the accuracy of a model  $h$  in our NAS search space  $H$ ,  $\text{MEM}$  is the TFLite memory footprint and  $\text{ENERGY}$  is the energy usage per inference of the network. Memory and energy usage are penalized with a ReLU function that activates after the thresholds,  $M_0$  and  $E_0$ , respectively, are crossed. We use an energy threshold of 1.25 mJ per inference, which is slightly more than 0.2% of the Pixel 4 XL battery when running once per second all day. Above the energy threshold,  $E_0$ , we explored two different slopes:  $b$  and  $b'$ . The harsher penalty  $b$ , is set to  $\frac{0.02}{0.75\text{mJ}}$ . Thus, above the energy threshold a 0.75 mJ increase in energy per inference must give at least a 2% increase in accuracy. The less harsh penalty sets  $b' = \frac{0.02}{1.75\text{mJ}}$ . We use a threshold,  $M_0$ , of 60 kB above which larger memory sizes are penalized with slope  $c = \frac{0.02}{30\text{kB}}$ . The 60 kB threshold is chosen to allow the network to be deployed on a wide variety of SRAM limited devices. The chosen slope means that a 90 kB model must have at least 0.02 accuracy points more than a 60 kB model for it to have a better reward. In the next five subsections, we discuss the quantized accuracy, measuring physical energy usage, approximate energy usage metrics, how we approximate energy usage during NAS using a random forest, and finally the memory usage in the reward function in Equation 1.

### 2.1 Quantized Accuracy

To measure the performance of the candidate architectures we use the accuracy of the 8-bit integer quantized TFLite model. The network is quantized using integer-8 quantization-aware training with the Tensorflow framework [3] to minimize the memory and

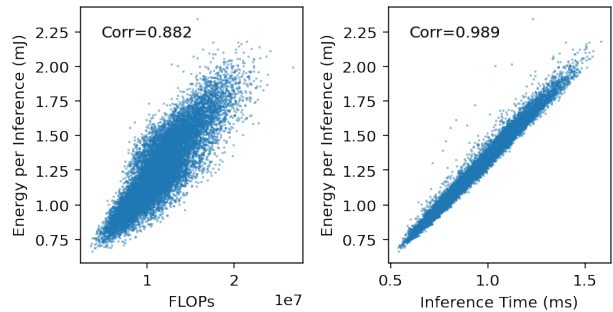


**Figure 3: Two approximations to the total energy consumption using FLOPs (left) and inference time (right).** These scatter plots are based on 15,000 randomly selected architectures in our search space measured on a Pixel 4 XL.

energy usage. There is generally good agreement between the non-quantized accuracy and the quantized accuracy (correlation of 0.955) but there are some outliers (up to 6.5% disagreement in accuracy) as seen in Figure 2. Since we are targeting on-device inference, we use the quantized accuracy in our reward function.

### 2.2 Physical Energy Measurements

We use a Monsoon power monitor [11] to measure the average power draw of a phone (without battery) running a candidate architecture. The energy per network inference is platform dependent, thus for this paper we focus on the big core CPU of the Pixel 4 XL. During the measurement, we lock the CPU core frequency and use a single thread. The average inference time is measured using the TFLite benchmarking tool. We use these energy measurements in three ways: to check the approximations others have used (Section 2.3), to train an approximate model to help guide the NAS (Section 2.4), and finally to verify the energy measurements shown in this paper (by repeating the measurement 5 times and reporting the mean).

### 2.3 Energy Approximations

Measuring energy usage of millions of network architectures is hard, but as we discuss above we have access to physical power measurements. Other papers have used FLOPs (total number of floating point operations of the unquantized model) or inference time (latency) to approximate energy usage [12, 14].

Figure 3 shows that a network with a FLOPs count of 10 million might use between 0.6 mJ per inference to 1.5 mJ per inference. This agrees with what several authors have reported that the FLOPs count is a poor proxy for energy usage on device, likely due to memory access not being accounted for in the FLOPs count [19].

Another approach to approximate energy usage is to consider the inference time of each network (sometimes called latency). We find the correlation between the average inference time and the average energy per inference (which is simply the average inference time multiplied by the average power) is 0.989 over our search space (Figure 3). Despite the good correlation, an average inference time of 0.85 ms could mean between 1.03 to 1.30 mJ per inference. The large spread of energy usage has to do with the fact that the average

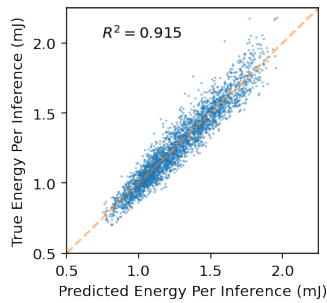


**Figure 4: Random forest model fit to the energy per inference of networks in the search space.**

power draw for each network in the search space is not the same, perhaps because some models use parallelism differently. Thereby, in the same unit of time, the CPU may work to a different level of its full capacity due to different degrees of parallel instructions.

## 2.4 Approximating Energy for NAS

To avoid the hardware difficulties of running every architecture Vizer suggests on a physical phone, we instead train a random forest (RF) model to predict the energy usage of models. Several other works model on device metrics, namely inference time, but no work the authors are aware of trains a model with on-device energy usage measurements directly [1]. The random forest model takes as input the architecture parameters (e.g. kernel sizes/filter types of each block) as well as model level parameters, total FLOPs count and the TFLite memory size. To train the RF model, we measure the average energy per inference of 15,000 architectures in our search space on the big core CPU of the Pixel 4 XL phone. The RF model has an  $R^2 = 0.92$  and RMSE of 0.07 mJ per inference (Figure 4). For reference, running a model with 1.3 mJ per inference from our search space five times on a pixel phone has an energy standard deviation (i.e. measurement noise) of 0.068 mJ. Since the RMSE of the RF model is close to the measurement noise from our phones, we feel confident using the predicted energy does not return significantly different NAS results compared to measuring energy usage for every network individually, and thus is a safe step in our NAS.

## 2.5 Memory Footprint

The SRAM available for small devices is somewhere between 10 kB to 1 MB and this memory is shared with multiple applications. In this search we use the TFLite executable size, i.e. the static memory of the application in our objective. We note that despite the parameter count being well correlated (0.942) to the quantized memory size of the network, it is still far from a perfect proxy. A parameter count of thirty thousand could mean anywhere between 50 to 65 kB of memory (Figure 2).

## 3 SEARCH SPACE

The art of neural architecture searches lies in efficiently exploring a good search space. A standard approach is to find a model that

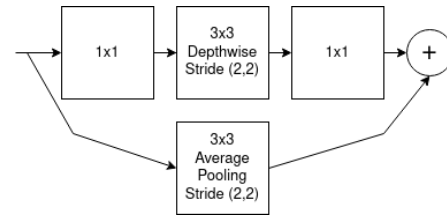


**Figure 5: MobileNetV2 Block with an Average Pooling Parallel Path when strides are (2,2). This block variation is called MobileNetV2-Avg-Pool and is inspired by ShuffleNet.**

achieves good performance on the dataset of interest and decompose that model into its component blocks [18]. We make use of MobileNetV1 [10] and MobileNetV2, which popularized depthwise separable convolutions, as benchmark models and use their two namesake block operations in our search space. We fix our network size to be twelve blocks. For every block, we search for the block type, the number of output filters, and convolution kernel size. Since the optimal parameters for each block is dependent on the position (e.g. a larger kernel is not so useful when the image size becomes very small towards the end of the network), we make the possible choices position dependent. Each of the twelve blocks has between nine to thirty options to choose from. In order to ensure the image size at the end of the network is the same for all possible candidates we fix the striding for all candidates to give a 7x5 image at the end of the network which is then fed into an average global pooling layer, before being fed into a constant 32 node dense layer that has 9 outputs (one for each class). We use a softmax activation on the logit outputs. The block macro-architecture is defined by the striding which is kept constant for each network and can be seen in Table 2. We visualize the search process in Figure 1.

### 3.1 KxK First Block

The input to the first block is a spectrogram with has no depth dimension. This means using a more expressive block like a KxK 2D convolution does not require a massive amount of computation. As such, like the MobileNet papers, we fix the first block type to be a KxK 2D Convolution, where K is the kernel size.

### 3.2 Second Block

The second block of our network is very important in terms of the computational load. The input to this block now has depth and as a result we fix this block type to be a Kx1 depthwise convolution followed by a 1xK depthwise convolution followed by a 1x1 pointwise convolution. We call this block the Kx1-1xK-DW block (where DW stands for depthwise). This is the least computationally intense block in our search space, hence the reason it is safe to choose for the second block of each network.

### 3.3 Other Blocks

The other ten blocks in our network use the block type choices of:

- MobileNetV1
- MobileNetV2
- Kx1-1xK-DW

- MobileNetV2-Avg-Pool (only for stride (2, 2))
- Identity (only for stride (1, 1)).
- Kx1-1xK (only for last block).

The last block of the network has a small input size and as a result we also introduce the block choice of a Kx1 convolution followed by a 1xK convolution. When the striding of a block is (1, 1), we also add the choice of the identity block. This is done to ensure the output image is always the same size of every architecture.

When using a striding of (2, 2), the original MobileNetV2 block does not contain a skip connection. The MobileNetV2 architecture is much larger than 12 blocks and most blocks in the original paper have a skip connection. Our network macro-architecture uses striding in five of the twelve blocks. We were motivated to add a parallel path to the MobileNetV2 block since we were worried information might be lost without it. We introduce a variation of the MobileNetV2 block, inspired by ShuffleNet named MobileNetV2-AvgPool, so that when the striding is (2, 2) the input to the block takes a parallel path through a 3x3 average pooling layer with stride of (2, 2) as can be seen in Figure 5 [22].

We experimented with squeeze and excite blocks such as the ones in MobileNetV3 [9]. We did not see any noticeable improvement in accuracy adding MobileNetV3 blocks, only increases in memory footprint and energy usage. As a result, we left these blocks out of our search space.

### 3.4 Kernel Sizes

We search for the kernel size among {3, 4, 5} for the first five blocks. After the fifth block the input image is 13x10 and as a result we fix the kernel size for later blocks to be 3.

### 3.5 Filter Sizes

We choose among three options for filters for every block in the network, these choices are position dependent. We use filter sizes that are a multiple of 8 since we saw energy usage increase when using filter sizes that were not multiples of 8 on the Pixel 4 XL CPU. With these filter choices approximately one quarter of the architectures in our search space have memory footprints smaller than 60 kB and energy usages of less than 1.25 mJ per inference.

### 3.6 1D Variant of the Search Space

We also ran a modification of this search space that reduces all block types to their one dimensional counterparts (e.g. KxK convolutional kernel becomes a Kx1 kernel). The input spectrogram to the network is transformed by swapping the frequency axis with the depth axis as was done in the TCResNet paper [4]. This modification reduces the overall computational requirements, so we expect low energy usage but we are uncertain whether the one dimensional variant of our search space will return similar accuracy to MobileNetV1/V2.

## 4 SOUND EVENT CLASSIFICATION DATASET

We use the AudioSet dataset which contains over 2 million human-annotated 10 second sound clips derived from YouTube videos [5]. The AudioSet ontology contains more than 500 classes, but we use a subset of them to limit the complexity of our task. Specifically, we chose labels that mimic Sound Notifications on Android. The 8

positive classes are (brackets indicate the original AudioSet labels, when multiple labels were mapped to one):

- Alarms (fire alarm, smoke alarm, CO alarm)
- Baby crying
- Dog barking (dog, bark, yip, howl, bow-wow, growling)
- Door knocking
- Doorbell (doorbell, ding-dong)
- Phone ringing
- Sirens (emergency vehicle, police car, ambulance, fire truck)
- Water running

We map all other classes in the AudioSet to a class labeled as the negative class. This tends to make this dataset somewhat challenging since the negative examples are all real sound events (e.g. guitar playing) and not simply low volume noise. In total we have 9 classes with one class being negative. We use the original train/evaluation/test split from AudioSet. We also ensure that our training/evaluation/test data is comprised of 50% negative class examples. The log-mel spectrogram of the data are computed and augmented with SpecAugment [15]. We believe this mapping of AudioSet is a representative task for always-on sound event classification, while the dataset is also large enough for a NAS study.

## 5 VIZIER SEARCH ALGORITHM

Our NAS is run on Vizier [6], a black-box optimization service that removes much of the software engineering work necessary to run and analyze NAS runs. Our NAS trains each network individually and employs early stopping to eliminate architectures unlikely to contend for a top final objective value [13]. The alternative approach in NAS, training a single super-network with all architecture possibilities present (weight-sharing) saves computational resources but there are no guarantees the ranking of individual networks using shared weights are valid [21]. Our search space consists of fairly small networks that take one tenth of the time to train compared to a larger network like MobileNetV2. As a result we opt for a more computationally intense search by training each sampled network individually to three quarters of the full training time with some networks that appear unpromising stopped early.

We employ two different search algorithms from Vizier for the NAS, one Bayesian and the other evolutionary, and run two thousand trials in each NAS experiment. Section 3 of Golovin’s [2017] paper describes the Bayesian algorithm. The evolutionary Hyper-Firefly algorithm is an extension of the Firefly algorithm which uses regularization and particle swarms [20]. The Firefly hyperparameters are tuned by another Firefly algorithm every 50 iterations, using an objective metric equal to the best objective value over a sliding window of 50 iterations.

Vizier’s Bayesian algorithm slows down considerably (i.e. requires more time to produce a new suggestion) for our search space after a thousand trials. This is because a Gaussian process algorithm has  $O(N^3)$  complexity, where N is the number of parameters multiplied by the number of trials. As a result, we switch from using the Gaussian process algorithm to the Hyper-Firefly algorithm after one thousand trials. Combining evolutionary algorithms with Bayesian approaches has been done before [21]. The results we obtain seem to generally favor the HyperFirefly (evolutionary) algorithm over the Bayesian (hybrid) algorithm. This could be due

to the evolutionary algorithm being more explorative for the first one thousand trials.

After training each sampled architecture on the training dataset, we evaluate the reward on the evaluation dataset. The architectures with best rewards are retrained five times for 33% longer on the same training set, and retested on the eval dataset. The best models from each NAS are retested with the unseen test dataset and these results are reported in this paper.

## 5.1 Early Stopping Algorithm

Vizier can decide to stop training a network early, if it finds it unpromising. After Vizier suggests an architecture to train, the memory size and the predicted energy of the architecture are sent back to Vizier. On top of that information, the model in training is periodically evaluated and the intermediate evaluation accuracy is sent back to Vizier. If Vizier’s early stopping model predicts that the current trial (architecture) will result in an objective worse than the best seen so far, with high confidence, the trial is stopped early. Early-stopping or performance curve stopping in Vizier is described in section 3.2 of Golovin’s paper [2017]. This rule uses a Gaussian Process (GP) with a custom kernel to regress the evaluation curves of all available trials, where each input feature to the GP is a time bucket in the time series.

Temporal spatial stopping (TSGP) learns a Gaussian Process model for each time series, using the exponential curve kernel ([17] Equation 6). The model also learns a mean function, at the asymptote, for each time series; and a mapping from the trial parameters to kernel parameters, allowing cross-trial information sharing. This allows Vizier to make automated stopping predictions about each time series, which are informed by both a strong exponential prior, and the trial parameters.

We compared no early stopping, exponential decaying early stopping with default parameters, and exponential decaying early stopping with TSGP learned parameters. Experimentation with the three methods return very similar rewards. The TSGP early stopping used the least amount of computation (50% less than forgoing early stopping) and as a result we employ it for our search.

## 6 RESULTS

Table 1 conveys energy usage, memory size and accuracy for the best NAS results and two types of baseline models: MobileNet and TCResNet. We include MobileNetV1/V2 as baseline models since they perform well on image classification tasks and are quite large models within our search space. The MobileNetV2 benchmark uses an expansion parameter of six. At the other end of the model size spectrum, we include TCResNet models which are known to perform well on speech command recognition and require low number of FLOPs and static memory. We use two different TCResNet model sizes, the TCResNet8 with width multiplier of one (labelled TCResNet8-1) and TCResNet14 with width multiplier of 1.5 (TCResNet14-1.5). Note, the benchmark models had to be slightly modified from their original paper version to work with a 196 by 40 size input since MobileNets are designed to run on square input images and the TCResNet is designed to run on a 96x40 size spectrogram. The baseline models are all quantized with the same int-8 quantization-aware training used in the NAS architectures. Table 1

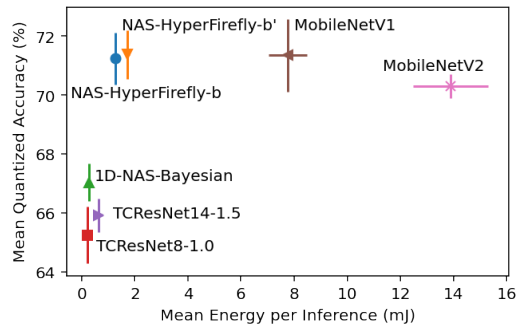


Figure 6: Mean energy per inference plotted against the mean quantized accuracy.

reports all models’ mean task accuracy after training five times to remove any bias from the initial starting condition. NAS done with the less harsh energy penalty  $b' = \frac{0.02}{1.75}$  is marked with an accent suffix (b’) in the Table. We visualize the NAS results from Table 1 in Figure 6.

NAS-HyperFirefly, the best network when using the less harsh energy penalty, achieves slightly worse accuracy than MobileNetV1 but better accuracy than MobileNetV2. Compared to MobileNetV2 it uses 50x less memory usage and 10x less energy usage. NAS-HyperFirefly-b’, which was run with a less harsh energy penalty than NAS-HyperFirefly, uses more energy than NAS-Firefly but also achieves better accuracy. NAS-HyperFirefly-b’ achieves slightly better mean accuracy than MobileNetV1, the baseline model with the best mean task accuracy.

The networks using one dimensional convolutions, as was done in TCResNet, in Table 1 tend to use very little energy but all return poor accuracy. 1D-NAS-Bayesian is the best NAS result when using only one dimensional convolutions. It achieves significantly better accuracy than both TCResNet baselines but with slightly more energy usage than TCResNet8-1.0.

The mean energy per inferences measured on the Pixel 4 XL CPU are not far from the predictions of the random forest model used during the NAS search. For example, the NAS-HyperFirefly uses 1.27 mJ on average where the RF prediction used by Vizier during the NAS was 1.35 mJ. Similarly, the NAS-HyperFirefly-b’ uses on average 1.72 mJ and the RF prediction was 1.69 mJ per inference.

## 7 DISCUSSION

Table 2 shows the best performing network structure found by NAS-Bayesian. Of interest is that the network uses the kernel size 5 twice in the network—the larger receptive field must allow the network to improve the task accuracy despite costing more computationally. The network uses both MobileNetV1 and V2 blocks and the new MobileNetV2-avg-pool and 1xK-Kx1-DW block we introduce in this paper. This block type heterogeneity agrees with what many NAS authors have found that it can be beneficial to have different types of block structures [2]. It also shows MobileNetV2 blocks are not always superior to MobileNetV1 blocks.

The number of output filters in the first block of the network creates a computational bottleneck when using 2D convolutions

**Table 1: NAS Results and Benchmarks. Top three models from each NAS are run five times against the test dataset and five times on a Pixel 4 XL CPU core for energy measurements.**

Model Name	Energy Per Inference (mJ)	TFLite Memory Size (kB)	Accuracy (%)	Inference Time (ms)	FLOPs	Parameters
NAS-Bayesian	1.30 ± 0.07	51.22	70.78 ± 0.78	0.98 ± 0.00	12.52M	23.95k
NAS-HyperFirefly	1.27 ± 0.07	53.61	71.24 ± 0.88	0.94 ± 0.00	13.26M	24.94k
NAS-Bayesian-b'	1.46 ± 0.08	56.96	70.89 ± 0.50	1.07 ± 0.01	10.95M	27.13k
NAS-HyperFirefly-b'	1.72 ± 0.07	45.10	71.38 ± 0.82	1.27 ± 0.01	15.61M	19.70k
1D-NAS-Bayesian	0.26 ± 0.01	55.38	67.04 ± 0.64	0.22 ± 0.00	6.43M	37.23k
MobileNetV2	13.90 ± 1.41	2717.83	70.30 ± 0.40	0.99 ± 0.04	430.35M	2301.18k
MobileNetV1	7.76 ± 0.71	3422.62	71.35 ± 1.23	5.47 ± 0.01	339.62M	3206.40k
TCResNet8-1.0	0.20 ± 0.01	78.69	65.23 ± 1.04	0.15 ± 0.01	6.00M	66.37k
TCResNet14-1.5	0.64 ± 0.06	331.06	65.91 ± 1.12	0.43 ± 0.00	26.24M	306.05k

**Table 2: Best NAS-Bayesian Model. Striding is the same for all 2D NAS models.**

Block Type	Kernel Size	Filters	Strides	FLOPs
KxK	5	8	(2, 1)	1.6M
1xK-Kx1-DW	3	24	(2, 1)	2.2M
1xK-Kx1-DW	3	32	(2, 2)	3.8M
MobileNetV1	3	32	(1, 1)	1.3M
MobileNetV2-Avg-Pool	5	24	(2, 2)	1.4M
MobileNetV2	3	24	(1, 1)	0.3M
Identity	-	-	(1, 1)	-
MobileNetV1	3	40	(1, 1)	0.2M
MobileNetV2	3	32	(1, 1)	0.9M
MobileNetV2	3	48	(2, 2)	0.4M
Identity	-	-	(1, 1)	-
MobileNetV1	3	64	(1, 1)	0.2M

on a spectrogram. Table 2 shows the FLOPs of each block in the optimum NAS-Bayesian network and we see the second block uses 2M FLOPs. This is despite the block having 8 input filters and using a kernel size of 3 and 24 output filters. If the number of input filters to the second block were instead 24, the FLOPs count would triple to 6M.

The computational burden of the first’s block number output of output filters is also seen in the energy usage of the network. The two most important features of our RF model that predicts energy are: the number of filters in 1st block (59%) and FLOPs (30%). The rest of the features had 2% or less impact. This shows the importance of the number of output filters used by the first block which creates a computational bottleneck in the network.

MobileNetV1 performs better than MobileNetV2 (expansion of 6) on this dataset. One of the main differences MobileNetV1 has to MobileNetV2 is a 1000 node dense embedding layer at the end of the network. The lack of the embedding layer may partly explain the poorer performance of MobileNetV2 which uses 700 kB less memory than MobileNetV1.

The NAS approach presented in this paper succeeds in finding a model (NAS-HyperFirefly) that is 10x more energy efficient and

gives an improvement in absolute mean accuracy of 0.94% compared to MobileNetV2. In comparison to MobileNetV1, we find a 4x more efficient network (NAS-HyperFirefly-b’) that uses more than 75x less memory and achieves 0.03% improvement in mean absolute accuracy.

We believe this approach of integrating on device energy usage into the NAS reward function is broadly applicable to other always-on tasks (e.g. video, IMUs). We also find 1D convolutional networks to be significantly more energy efficient but poor in task accuracy. For use cases where even less energy per inference is targeted, we suggest further research into expanding the search space to use 1D convolutional blocks and/or combining this approach with model compression techniques (e.g. weight pruning).

## ACKNOWLEDGMENTS

We thank our colleagues: Chansoo Lee, Hassan Rom, Kevin Kilgour, Marco Tagliasacchi, Mathieu Parvaix, Daniel Ellis, Gabriel Bender, Quoc Le, Pete Warden, Merve Kaya, Grace Chu and Jason Rugolo for their advice.

## REFERENCES

- [1] Gabriel Bender, Hanxiao Liu, Bo Chen, Grace Chu, Shuyang Cheng, Pieter-Jan Kindermans, and Quoc V Le. 2020. Can Weight Sharing Outperform Random Architecture Search? An Investigation with TuNAS. In *Proceedings of the IEEE/CVF Conference on Computer Vision and Pattern Recognition*. 14323–14332.
- [2] Han Cai, Ligeng Zhu, and Song Han. 2018. Proxylessnas: Direct Neural Architecture Search on Target Task and Hardware. *arXiv preprint arXiv:1812.00332* (2018).
- [3] Alan Chiao and Frédéric Rechtenstein. 2021. *Quantization aware training comprehensive guide*. Retrieved December 12, 2021 from [https://www.tensorflow.org/model\\_optimization/guide/quantization/training\\_comprehensive\\_guide](https://www.tensorflow.org/model_optimization/guide/quantization/training_comprehensive_guide)
- [4] Seungwoo Choi, Seokjun Seo, Beomjun Shin, Hyeonmin Byun, Martin Kersner, Beomsu Kim, Dongyoung Kim, and Sungjoo Ha. 2019. Temporal Convolution for Real-Time Keyword Spotting on Mobile Devices. *arXiv preprint arXiv:1904.03814* (2019).
- [5] Jort F Gemmeke, Daniel PW Ellis, Dylan Freedman, Aren Jansen, Wade Lawrence, R Channing Moore, Manoj Plakal, and Marvin Ritter. 2017. Audio Set: An Ontology and Human-Labeled Dataset for Audio Events. In *2017 IEEE International Conference on Acoustics, Speech and Signal Processing (ICASSP)*. IEEE, 776–780.
- [6] Daniel Golovin, Benjamin Solnik, Subhodeep Moitra, Greg Kochanski, John Karro, and David Sculley. 2017. Google Vizier: A Service for Black-Box Optimization. In *Proceedings of the 23rd ACM SIGKDD International Conference on Knowledge Discovery and Data Mining*. 1487–1495.
- [7] Kaiming He, Xiangyu Zhang, Shaoqing Ren, and Jian Sun. 2016. Deep Residual Learning for Image Recognition. In *Proceedings of the IEEE Conference on Computer Vision and Pattern Recognition*. 770–778.
- [8] Shawn Hershey, Sourish Chaudhuri, Daniel PW Ellis, Jort F Gemmeke, Aren Jansen, R Channing Moore, Manoj Plakal, Devin Platt, Rif A Saurous, Bryan Seybold, et al. 2017. CNN architectures for Large-Scale Audio Classification. In *2017 IEEE International Conference on Acoustics, Speech and Signal Processing (ICASSP)*. IEEE, 131–135.
- [9] Andrew Howard, Mark Sandler, Grace Chu, Liang-Chieh Chen, Bo Chen, Mingxing Tan, Weijun Wang, Yukun Zhu, Ruoming Pang, Vijay Vasudevan, et al. 2019. Searching for MobileNetV3. In *Proceedings of the IEEE/CVF International Conference on Computer Vision*. 1314–1324.
- [10] Andrew G Howard, Menglong Zhu, Bo Chen, Dmitry Kalenichenko, Weijun Wang, Tobias Weyand, Marco Andreetto, and Hartwig Adam. 2017. Mobilenets: Efficient Convolutional Neural Networks for Mobile Vision Applications. *arXiv preprint arXiv:1704.04861* (2017).
- [11] Monsoon Solutions Inc. 2021. *Monsoon Power Monitor Manual*. Retrieved December 12, 2021 from <http://msoon.github.io/powermonitor/PowerTool/doc/Power%20Monitor%20Manual.pdf>
- [12] Jixiang Li, Chuming Liang, Bo Zhang, Zhao Wang, Fei Xiang, and Xiangxiang Chu. 2019. Neural Architecture Search on Acoustic Scene Classification. *arXiv preprint arXiv:1912.12825* (2019).
- [13] Liam Li and Ameet Talwalkar. 2020. Random search and reproducibility for neural architecture search. In *Uncertainty in artificial intelligence*. PMLR, 367–377.
- [14] Bingqian Lu, Jianyi Yang, Weiwen Jiang, Yiyu Shi, and Shaolei Ren. 2021. One Proxy Device Is Enough for Hardware-Aware Neural Architecture Search. *arXiv preprint arXiv:2111.01203* (2021).
- [15] Daniel S Park, William Chan, Yu Zhang, Chung-Cheng Chiu, Barret Zoph, Ekin D Cubuk, and Quoc V Le. 2019. SpecAugment: A Simple Data Augmentation Method for Automatic Speech Recognition. *arXiv preprint arXiv:1904.08779* (2019).
- [16] Mark Sandler, Andrew Howard, Menglong Zhu, Andrey Zhmoginov, and Liang-Chieh Chen. 2018. MobileNetV2: Inverted Residuals and Linear Bottlenecks. In *Proceedings of the IEEE conference on computer vision and pattern recognition*. 4510–4520.
- [17] Kevin Swersky, Jasper Snoek, and Ryan Prescott Adams. 2014. Freeze-thaw Bayesian optimization. *arXiv preprint arXiv:1406.3896* (2014).
- [18] Bichen Wu, Xiaoliang Dai, Peizhao Zhang, Yaghan Wang, Fei Sun, Yiming Wu, Yuandong Tian, Peter Vajda, Yangqing Jia, and Kurt Keutzer. 2019. FBNet: Hardware-Aware Efficient Convnet Design via Differentiable Neural Architecture Search. In *Proceedings of the IEEE/CVF Conference on Computer Vision and Pattern Recognition*. 10734–10742.
- [19] Tien-Ju Yang, Andrew Howard, Bo Chen, Xiao Zhang, Alec Go, Mark Sandler, Vivienne Sze, and Hartwig Adam. 2018. NetAdapt: Platform-Aware Neural Network Adaptation for Mobile Applications. In *Proceedings of the European Conference on Computer Vision (ECCV)*. 285–300.
- [20] Xin-She Yang. 2010. *Nature-Inspired Metaheuristic Algorithms*. Luniver press.
- [21] Yao Yang, Andrew Nam, Mohamad Nasr-Azadani, and Teresa Tung. 2020. Resource-Aware Pareto-Optimal Automated Machine Learning Platform. In *2020 3rd International Seminar on Research of Information Technology and Intelligent Systems (ISRITI)*. IEEE, 1–6.
- [22] Xiangyu Zhang, Xinyu Zhou, Mengxiao Lin, and Jian Sun. 2018. ShuffleNet: An Extremely Efficient Convolutional Neural Network for Mobile Devices. In *Proceedings of the IEEE conference on computer vision and pattern recognition*. 6848–6856.